RESEARCH ARTICLE
doi: 10.2306/scienceasia1513-1874.2022.130

ScienceAsia 49 (2023): **56–62**

The role of the phosphatidylinositol 3-kinase/protein kinase B signaling pathway in the pulmonary vascular remodeling of pulmonary arterial hypertension in rats

Yan Duan[a,b], **Ting Wang**[a,b], **Shan-Shan Wu**[c], **Dong Liu**[a,b], **Jian Zhao**[a,b], **Bin Liu**[a,b,*]

[a] Department of Pediatrics, the Affiliated Hospital of Southwest Medical University, Jiangyang, Luzhou 646000 China
[b] Sichuan Clinical Research Center for Birth Defects, China
[c] Department of Emergency Medicine, West China Second Hospital of Sichuan University, Chengdu 610041 China

*Corresponding author, e-mail: lblyfy@126.com

Received 13 Oct 2021, Accepted 27 Jun 2022
Available online 10 Oct 2022

ABSTRACT: This study aimed to investigate the role of the phosphatidylinositol 3-kinase/protein kinase B (PI3K/Akt) signaling pathway in the pulmonary vascular remodeling (PVR) of pulmonary arterial hypertension (PAH) in rats. A PAH model in rats was established through a left pneumonectomy and monocrotaline (MCT) injection, using the transglutaminase 2 (TG2) inhibitor cystamine dihydrochloride for intervention. Thirty healthy male Sprague Dawley rats were randomized into a control group, a model group, and an intervention group ($n = 10$ for each group). The mean pulmonary arterial pressure (mPAP) was measured in all groups after 35 days, and the right ventricular hypertrophy index (RVHI) was calculated. Hematoxylin and eosin and lung elastic-fiber staining were used on the rats' lung tissue in all three groups. The changes in pulmonary blood vessels and lung tissue force and the percentage of medial hypertrophy of small pulmonary arteries (WT%), vessel wall area to total area ratio (WA%), and the neointimal proliferation degree were observed. The Akt messenger RNA (mRNA) expression levels of lung tissues in all three groups were measured using a real-time polymerase chain reaction (RT-PCR) assay, and the protein expression levels of Akt and phosphorylated Akt (p-Akt) in all three groups were measured using a Western blot assay. The results indicated that the PI3K/Akt signaling pathway might play a substantial role in inhibiting pulmonary vascular remodeling (PVR) following intervention with a TG2 inhibitor.

KEYWORDS: pulmonary vascular remodeling, PAH, TG2, cell signaling

INTRODUCTION

PAH is a progressive disorder characterized by high blood pressure (hypertension) in the arteries of the lungs (pulmonary artery), eventually resulting in death due to right heart failure [1]. Pathological studies have found that PVR is the most important pathological feature of PAH [2]. However, the diagnosis for patients with PAH is often challenging, as there is no precise and effective treatment regime, and the pathogenesis remains unclear.

The PI3K/Akt signaling pathway widely exists in cells. Currently, most studies focus on its role in the occurrence and the development of tumors [3, 4]. It is abnormally activated in many malignant tumors, and the activated product combines with Akt to change its conformation. PI3K promotes the phosphorylation of Akt at Thr308 by 3-phosphoinositol-dependent protein kinase-1, leading to the activation of Akt into p-Akt with phosphokinase activity [5]. Recent studies [6–8] have shown that the PI3K/Akt signaling pathway is involved in the regulation of the proliferation, migration, and apoptosis of pulmonary artery smooth muscle cells (PASMCs) and pulmonary vascular endothelial cells; thus, the pathway plays an essential role in vascular remodeling.

Recent studies have shown that TG2 is involved in PVR in PAH [9, 10]. However, its mechanism of action remains unclear. The PI3K/Akt signaling pathway is an anti-apoptotic signaling pathway. Studies [11] have shown that the activation of TG2 expression can subsequently activate the PI3K/Akt signaling pathway, resulting in uncontrolled cell growth. In the MCT induced rat pulmonary hypertension animal model, the Akt signaling pathway is involved in PVR [12]. Cystamine dihydrochloride is a unique competitive amine TG2 inhibitor with irreversibility [13]. In the present study, a PAH animal model was established using left pneumonectomy and MCT injection. The TG2 inhibitor cystamine dihydrochloride was used as an intervention, and the Akt gene and protein expression changes were observed. Based on previous studies, the prevention of PAH formation using TG2 inhibitors was continuously investigated in order to identify if this intervention was related to the activation of the PI3K/Akt signaling pathway.

MATERIALS AND METHODS

Laboratory animals

Thirty clean-grade healthy male Sprague Dawley rats, aged 6–8 weeks and weighing 300–350 g, were used for this study. This study was conducted with approval from the Ethics Committee of The Affiliated Hospital of

Southwest Medical University.

All animals were treated in compliance with the National Research Council's Guide for the Care and Use of Laboratory Animals (1996).

Establishment of the pulmonary arterial hypertension animal model

A PAH animal model of rats was established by establishing left pneumonectomy and MCT injection, according to Wang et al [14]. The rats were randomly separated into three groups of ten: control, model, and intervention groups. According to the modeling method, the control group received no intervention, and the model group underwent left pneumonectomy with MCT (Sigma Company, USA) (60 mg/kg) injected subcutaneously into the back on day seven after surgery [15]. The intervention group underwent left pneumonectomy and MCT injection in the same way as the model group but received an intraperitoneal injection of cystamine dihydrochloride (Sigma Company) (112 mg/kg) once daily from day five after surgery [16] until day 35. The rats in all groups were allowed to take water and food freely. They were euthanized after the mPAP was measured on day 35, then the tissue samples of their right lungs were collected.

Detection of hemodynamic indexes

The mPAP was recorded as the Ref. [17]. Tissue samples from the right lung and the entire heart were taken from each rat. The free wall of the right ventricle (RV), the left ventricle (LV), and the interventricular septum (LV + S) were separate; and the ratio (RV/[LV+S]) was calculated after weighing to obtain the RVHI.

Detection of the histopathological indexes of the lung

The right lung tissue samples were routinely embedded in paraffin, and sections were made for hematoxylin and eosin (H&E) and elastic-fiber staining. Ten fields in each H&E-stained section were randomly observed, with pulmonary arterioles of a diameter $\leqslant$150 μm as the observation objects. The neointimal formation on the outer sides of the inner elastic plate and the endothelial cells was observed, and the number of blood vessels with neointimal formation was counted. Between 30 and 40 pulmonary arterioles were randomly observed per section. The proliferation of neointima was calculated: proliferation of neointima (%) = (the number of blood vessels with neointimal formation/the total number of observed blood vessels) × 100%.

Images were processed with ImagePro Plus software, and the total area, the wall area, the circumference of the midline, the blood vessel thickness, and the inner and the outer diameters of the blood vessels were investigated. Approximately 15–20 small vessels were observed in each section, and the average value was calculated. The calculations were as follows: media thickness (MT) of blood vessel = cross-sectional wall area/the circumference on midline; vascular radius = circumference on midline/2π; intravascular (external) diameter = vascular radius − (+) thickness; WT% = (MT of pulmonary arteriole/vascular outer diameter) × 100%; and WA% = (vascular wall area/-total vascular area) × 100%.

Measurement of protein kinase messenger RNA expression levels using RT-PCR

The lung tissues were removed from the rat and frozen, and the instructions for TRIzol (BIOWEST Company, France) were used to test the integrity of the RNA using agarose gel electrophoresis.

The RNA was reversely transcribed into complementary DNA (cDNA) for PCR amplification using random primers and reverse transcriptase. The amplified target gene was designed with primers based on the gene sequence of rat Akt in the National Center for Biotechnology Information gene database. β-actin was used as the internal reference, and the primers were synthesized by a company (TaKaRa, Japan). The quality qualification test was passed.

The relative expression of the target gene was calculated using ΔCt. The relative expression of the target gene = $2^{-\Delta\Delta Ct}$, with $2^{-\Delta\Delta Ct}$ representing the fold of the relative expression of the target gene in relation to the control group. ΔΔCt was the final quantitative result for statistical analysis.

Analysis of protein kinase and phosphorylated protein kinase activity in lung tissues using western blotting

The frozen lung tissues were removed to extract the protein following the TRIzol instructions, and the protein content was measured using bicinchoninic acid assay and sodium dodecyl sulfate-polyacrylamide gel electrophoresis. The band diagram was measured and analyzed for band density using ImageJ software. The relative expression level of the target protein = the band density of the target protein/the band density of the internal reference protein. In this study, tubulin was used as the internal reference protein.

Statistical analysis

All data obtained in this study were expressed as mean ± standard deviation (SD). The data in each group were analyzed using SPSS 20.0 software, and a one-way analysis of variance was used for statistical analysis. The mean between the groups was compared using Fisher's least significant difference method. $p < 0.05$ was considered statistically significant.

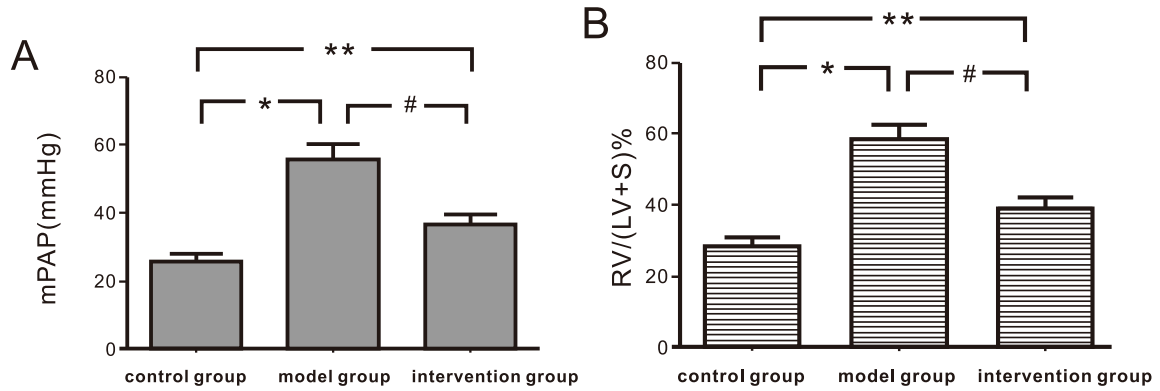

Fig. 1 Comparison of the mPAP and RVHI of the rats in control, model, and intervention groups: A, the mPAP; B, the RVHI.

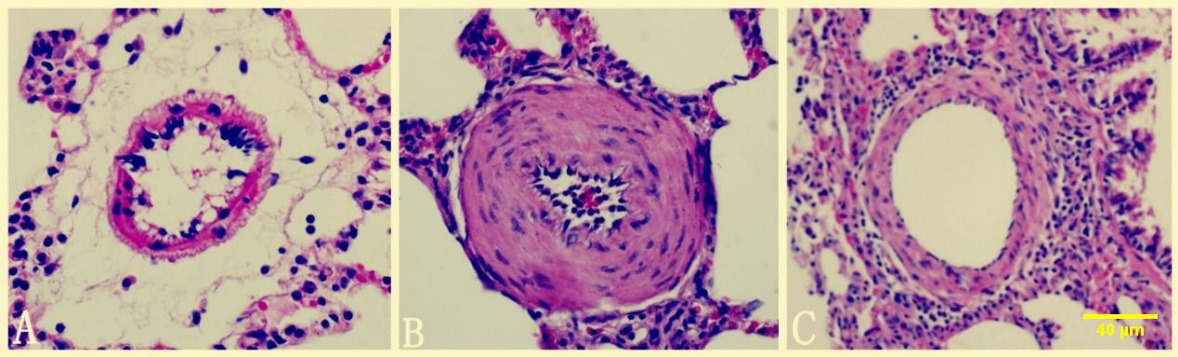

Fig. 2 Hematoxylin-eosin staining (× 400) of the lung tissue from rats in: A, control group; B, model group; C, intervention group.

RESULTS

General conditions of the rats in each group

Rats in the three groups were raised in the same environment. During the study, it was observed that rats in the model group gradually developed decreased food intake and activity, slow reactions, weight loss, tachypnea, and wheezing, with symptoms becoming progressively aggravated; in some cases, hepatomegaly, heart failure, and death occurred. These symptoms also occurred in some rats in the intervention group but with less severity, and fewer deaths occurred. Rats in the control group remained in good condition, with no obvious characterization of the above symptoms, and no deaths occurred.

As shown in Fig. 1, the mPAP and (RV/[LV + S]) of the rats in the model group were 55.92 ± 4.30 and 57.60 ± 3.62; and in the control group, they were 25.31 ± 2.68 and 28.24 ± 2.16, respectively, with a statistically significant difference ($p < 0.05$) After intervention with cystamine dihydrochloride, the mPAP and (RV/[LV + S]) in the intervention group were 36.55 ± 2.80 and 38.30 ± 3.11, significantly lower than in the model group, which were 55.92 ± 4.30 and 57.60 ± 3.62 ($p < 0.05$), respectively.

Comparison and morphological observations of lung tissues of the rats in each group

Hematoxylin and eosin-stained sections of lung tissues

As shown in Fig. 2, the wall thickness of the pulmonary arterioles in the rats in the model group was significantly increased. The lumen became narrowed; and in some cases, part of the lumen was completely occluded. Besides, more inflammatory cell infiltration was observed around vessels in the model group. The wall thickness of the pulmonary arterioles of the rats in the intervention group was increased compared with the control group but significantly reduced compared with the model group. In contrast, the pulmonary arterioles of the rats in the control group had relatively thin walls and large lumens with no occlusion.

Elastic-fiber-stained sections of lung tissues

Fig. 3 and Fig. 4 show that the internal and external elastic lamella, the vascular lumen of the pulmonary arterioles, and the vascular wall between the internal and external elastic lamella were clearly observed. In the model group, the wall thickness of the pulmonary arterioles was significantly increased, with the lumen

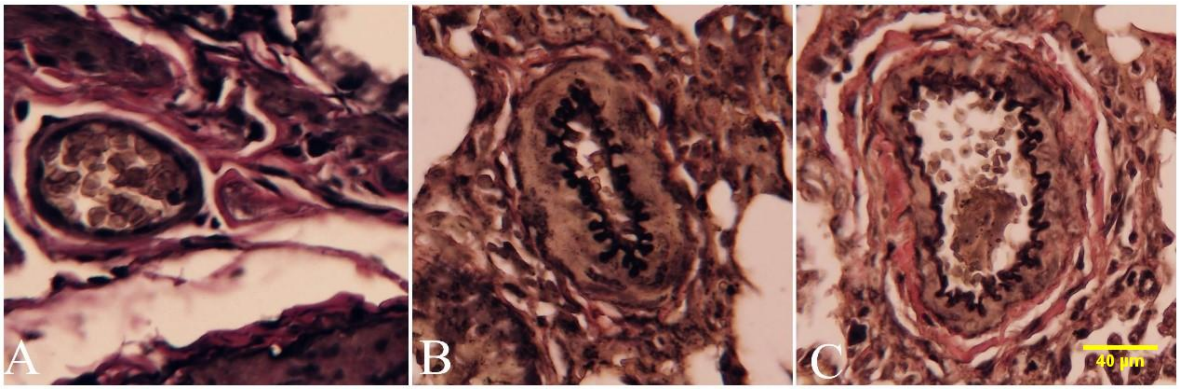

Fig. 3 Elastin Van Gieson staining (× 400) of the small pulmonary artery of rats in: A, control group; B, model group; C, intervention group.

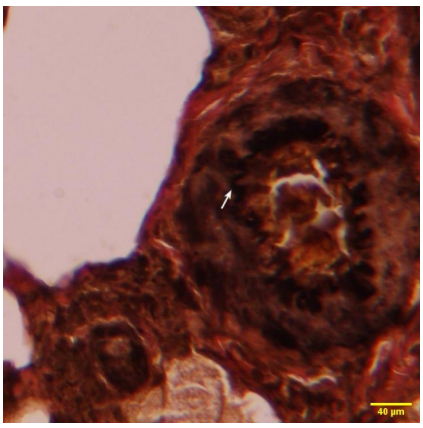

Fig. 4 Neointimal formation in model group (Elastin-Van Gieson staining, × 400). The arrow points to the neointima.

significantly narrowed. The neointima formation was observed on the medial side of the elastic lamella. The wall thickness of the pulmonary arterioles in the rats in the intervention group was also increased, with a narrowed lumen. The neointima formation was observed on the medial side of some elastic lamella in the intervention group, with less severity than in the model group. There was no obvious thickening of the pulmonary arteriole walls and no neointima formation in the control group.

As shown in Fig. 5, the neointima proliferation of the pulmonary arterioles, WA%, and WT% in the model group were 58.08 ± 3.98, 69.80 ± 5.28, and 43.70 ± 5.11, respectively. After intervention with cystamine dihydrochloride, the neointima proliferation of the pulmonary arterioles, WA%, and WT% in the intervention group were 28.00 ± 4.02, 47.82 ± 3.75, and 29.11 ± 3.50, respectively, which were significantly lower than the model group ($p < 0.05$). No neointimal formation was observed in the control group. The WA% and WT% in the control group were 28.81 ± 3.13 and 19.64 ± 3.23, respectively, which were all lower than the other two groups, and the differences were statistically significant.

As shown in Fig. 6, the relative expression levels of Akt mRNA in the model group were 2.07 ± 0.21, significantly higher than in the control group, which were 1.06 ± 0.17 ($p < 0.05$). After intervention with cystamine dihydrochloride, the relative expression levels of Akt mRNA in the intervention group were 1.49 ± 0.15, which was significantly lower than in the model group ($p < 0.05$).

Comparison of the protein expression levels of Akt and p-Akt in the lung tissues in all groups

As shown in Fig. 7, the protein expression levels of Akt and p-Akt in the lung tissues of the rats in the model group were 1.44 ± 0.15 and 1.07 ± 0.14, respectively, which were significantly higher than in the control group, which were 0.59 ± 0.12 and 0.47 ± 0.07 ($p < 0.05$). After intervention with cystamine dihydrochloride, the protein expression levels of Akt and p-Akt in the lung tissues of the rats in the intervention group were 1.02 ± 0.13 and 0.73 ± 0.11, respectively, which were significantly lower than in the model group ($p < 0.05$).

DISCUSSION

In this study, we found that the mPAP, RVHI%, WT%, WA%, and degree of neointimal proliferation in the intervention group were significantly decreased after the PI3K/Akt signaling pathway was inhibited by cystamine dihydrochloride. Furthermore, the expression levels of Akt mRNA and the protein expression levels of Akt and p-Akt in the intervention group were significantly lower than in the model group. The PAH model in rats was successfully established using left pneumonectomy and an MCT injection, with neointimal proliferation and typical pathological characteristics of PVR. The use of the TG2 inhibitor cystamine

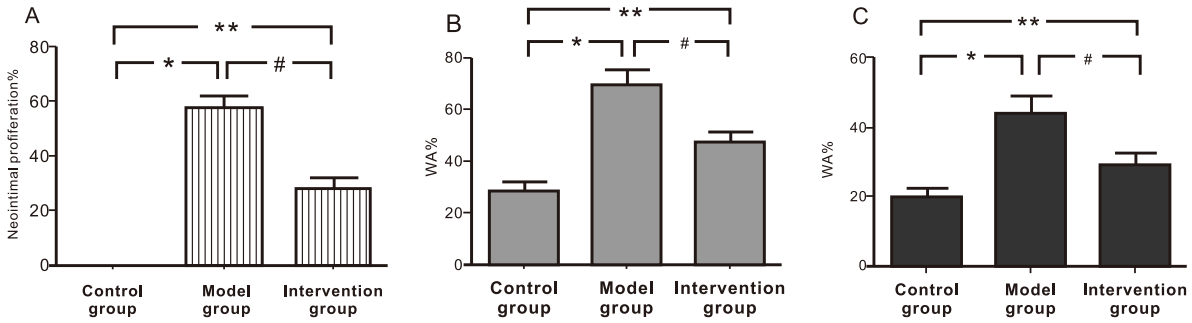

Fig. 5 Comparison of: A, the neointimal proliferation of the pulmonary arterioles; B, the WA%; and C, the WT% of rats in the three groups.

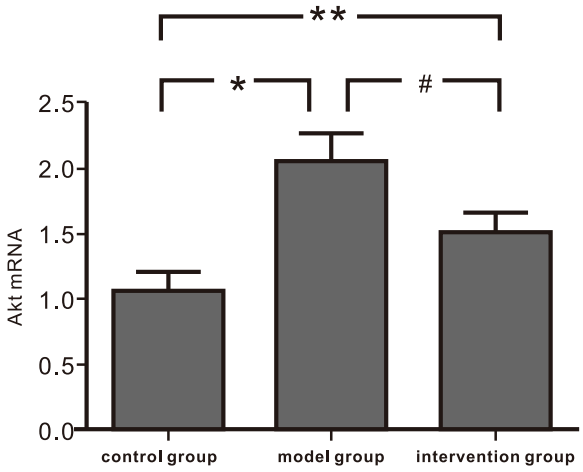

Fig. 6 Comparison of the relative expression levels of Akt mRNA in the lung tissues of rats in the three groups.

dihydrochloride suppressed the formation of PAH to some extent and blocked PVR.

A PAH may be a disease, but it can also exist as a complication or a syndrome. Although further research were conducted in recent decades, leading to significant progress, the pathogenesis of PAH remains unclear; and further investigation and effective measures for its prevention and treatment are required. Therefore, establishing a suitable PAH animal model has been the basis for all studies.

Pulmonary vascular remodeling is vital in the formation of PAH. It includes intracellular injury and the proliferation of smooth muscle cells, leading to increased MT, myotization of small arteries without smooth muscles, and further myotization of muscular pulmonary arteries, resulting in progressive vascular occlusion, neointimal formation, and formation of plexiform lesions [18].

In the present study, left pneumonectomy and an MCT injection were administered for modeling. The results showed the successful establishment of a PAH animal model by left pneumonectomy and MCT injection, with good stimulation for changes of severe PAH characterized by PVR. This animal model would be suitable for further study and drug intervention trials for the pathogenesis of PAH and PVR with neointimal formation. The results reported by Nishimura et al [19] were consistent with the present study. Our previous studies comparing the establishment of a PAH animal model using four different methods (an abdominal aortocaval shunt, a left pneumonectomy, an MCT resection, and a left pneumonectomy with MCT injection) also confirmed the above results [17].

The TG2 is widely present in a variety of cells, including endothelial cells, smooth muscle cells, and immune-related cells. The TG2 is a multifunctional protein that catalyzes the formation of covalent bonds cross-linking between proteins to complete the protein post-translational modifications. It is also involved in the occurrence and development of many diseases by activating multiple signaling pathways. Recently, the TG2 was reported involving in the formation of PAH through the serotonin reuptake mechanism, which was related to PVR [9, 10, 20, 21]. However, the specific mechanism of TG2 remains unclear. In the present study, the TG2 inhibitor cystamine dihydrochloride was used as an intervention. The results showed that the TG2 inhibitor could inhibit the formation of pulmonary hypertension to a certain extent, which were consistent with those of previous studies [14].

Previous studies have reported that by inhibiting the activation of the PI3K/Akt signaling pathway in hypoxic PAH, the proliferation of hypoxia-induced vascular smooth muscle cells was inhibited, thereby inhibiting the vascular remodeling [22, 23]. Teng et al [24] confirmed that a hypoxia-induced mitogenic factor (HIMF) could be activated by phosphorylating Akt into p-Akt. It was also found that when p-Akt decreased, the proliferation of PASMCs was reduced. Moreover, the degree of pulmonary vasoconstriction was lowered when PI3K and HIMF recombinant protein inhibitors were added, indicating that the PI3K/Akt signaling pathway was involved in the proliferation of smooth

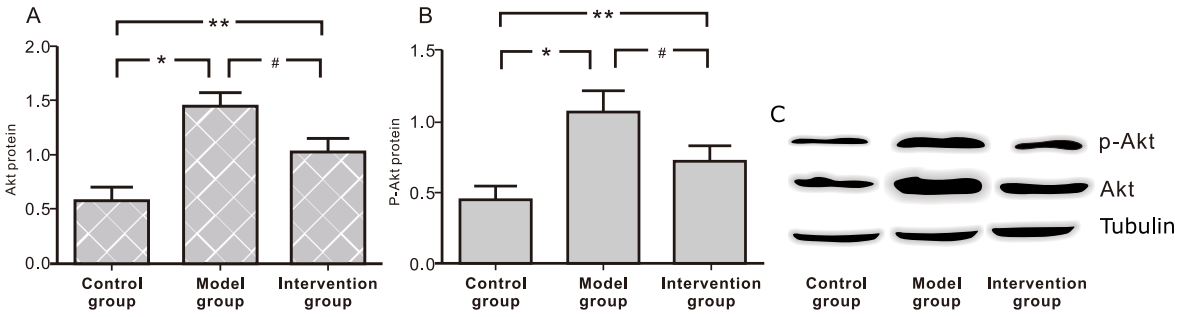

Fig. 7 Comparison of: A, expression of Akt protein; B, expression of p-Akt protein; C, comparison of the expression of Akt and p-Akt protein of the lung tissue from rats in the three groups.

muscle cells induced by a HIMF. Therefore, the present study assumed that the PI3K/Akt signaling pathway was involved in the inhibition of PVR by the TG2 inhibitor.

This study showed that the expression levels of Akt mRNA, Akt, and p-Akt proteins in the lung tissues of rats in the model group were significantly increased. After intervention with cystamine dihydrochloride, these indexes were all reduced, indicating that the inhibition of PVR by the TG2 signaling pathway prevented the formation of PAH to some extent. Based on what reported in previous studies that the TG2 inhibitor monodansylcadaverine (MDC) inhibited the proliferation of PASMCs induced by 5-HT, Penumatsa et al [25] continued to study the mechanisms of the inhibition of proliferation and found that TG2 catalyzed the covalent bonding between 5-HT and Akt to form serotonergic Akt, resulting in the activation of Akt and its downstream signaling targets (mammalian target of rapamycin (mTOR), s6 kinase, and s6) leading to the proliferation of PASMCs induced by 5-HT. This process could be inhibited by MDC, indicating that the Akt signaling pathway was involved in the proliferation of PASMCs induced by 5-HT, which was consistent with the results of the present study. Other studies [11] have also found that the selective 5-HT reuptake inhibitor fluoxetine can inhibit MCT-induced PVR in rats through the Rho/ROCK and Akt signaling pathways.

The current study had some limitations; for example, the downstream molecules of Akt were not investigated. The study found many effector molecules downstream of Akt, whose activation or inhibition could guide the cascade reactions of the signal transduction pathways to play a role in the regulation of cell proliferation and differentiation, glucose metabolism, protein synthesis, and other biological activities. So further investigation and improvement of the related index assays are required.

CONCLUSION

This study preliminarily investigated the effects and molecular mechanisms of TG2 inhibitors on the PVR of PAH in rats. The results of the study indicated that the PI3K/Akt signaling pathway might play a substantial role in inhibiting PVR after an intervention with a TG2 inhibitor. The finding could be a potential strategy for PAH treatment.

REFERENCES

1. Nef HM, Möllmann H, Hamm C, Grimminger F, Ghofrani HA (2010) Pulmonary hypertension: updated classification and management of pulmonary hypertension. *Heart* **96**, 552–559.
2. Jeffery TK, Morrell NW (2002) Molecular and cellular basis of pulmonary vascular remodeling in pulmonary hypertension. *Prog Cardiovasc Dis* **45**, 173–202.
3. Tao R, Wang F, Feng X, Yang W (2022) miR-10a-5p inhibits the migration and invasion of human oral carcinoma cells by targeting PIK3CA through PI3K/AKT/mTOR pathway. *ScienceAsia* **48**, 538–544.
4. Guan J, Huang H (2022) Chrysophanol induces cell apoptosis and suppresses cell invasion by regulating AKT and MAPK signaling pathway in melanoma cells. *ScienceAsia* **48**, 558–567.
5. Fresno Vara JA, Casado E, de Castro J, Cejas P, Belda-Iniesta C, González-Barón M (2004) PI3K/Akt signalling pathway and cancer. *Cancer Treat Rev* **30**, 193–204.
6. Li L, Xu M, Li X, Lv C, Zhang X, Yu H, Zhang M, Fu Y, et al (2015) Platelet-derived growth factor-B (PDGF-B) induced by hypoxia promotes the survival of pulmonary arterial endothelial cells through the PI3K/Akt/Stat3 pathway. *Cell Physiol Biochem* **35**, 441–451.
7. Li S, Li Q, Lv X, Liao L, Yang W, Li S, Lu P, Zhu D (2015) Aurantio-obtusin relaxes systemic arteries through endothelial PI3K/AKT/eNOS-dependent signaling pathway in rats. *J Pharmacol Sci* **128**, 108–115.
8. Wei C, Li HZ, Wang YH, Peng X, Shao HJ, Li HX, Bai SZ, Lu XX, et al (2016) Exogenous spermine inhibits the proliferation of human pulmonary artery smooth muscle cells caused by chemically-induced hypoxia via the suppression of the ERK1/2- and PI3K/AKT-associated pathways. *Int J Mol Med* **37**, 39–46.
9. Penumatsa KC, Toksoz D, Warburton RR, Hilmer AJ, Liu T, Khosla C, Comhair SA, Fanburg BL (2014) Role of hypoxia-induced transglutaminase 2 in pulmonary artery smooth muscle cell proliferation. *Am J Physiol Lung Cell Mol Physiol* **307**, L576–L585.

10. DiRaimondo TR, Klöck C, Warburton R, Herrera Z, Penumatsa K, Toksoz D, Hill N, Khosla C, et al (2014) Elevated transglutaminase 2 activity is associated with hypoxia-induced experimental pulmonary hypertension in mice. *ACS Chem Biol* **9**, 266–275.
11. Wang HM, Wang Y, Liu M, Bai Y, Zhang XH, Sun YX, Wang HL (2012) Fluoxetine inhibits monocrotaline-induced pulmonary arterial remodeling involved in inhibition of RhoA-Rho kinase and Akt signalling pathways in rats. *Can J Physiol Pharmaco* **l90**, 1506–1515.
12. Verma A, Wang H, Manavathi B, Fok JY, Mann AP, Kumar R, Mehta K (2006) Increased expression of tissue transglutaminase in pancreatic ductal adenocarcinoma and its implications in drug resistance and metastasis. *Cancer Res* **66**, 10525–10533.
13. Siegel M, Khosla C (2007) Transglutaminase 2 inhibitors and their therapeutic role in disease states. *Pharmacol Ther* **115**, 232–245.
14. Wang T, Duan Y, Liu D, Li G, Liu B (2022) The effect of transglutaminase-2 inhibitor on pulmonary vascular remodeling in rats with pulmonary arterial hypertension. *Clin Exp Hypertens* **44**, 167–174.
15. Schermuly RT, Kreisselmeier KP, Ghofrani HA, Yilmaz H, Butrous G, Ermert L, Ermert M, Weissmann N, et al (2004) Chronic sildenafil treatment inhibits monocrotaline-induced pulmonary hypertension in rats. *Am J Respir Crit Care Med* **169**, 39–45.
16. Qiu JF, Zhang ZQ, Chen W, Wu ZY (2007) Cystamine ameliorates liver fibrosis induced by carbon tetrachloride via inhibition of tissue transglutaminase. *World J Gastroenterol* **13**, 4328–4332.
17. Zhao J, Yang MF, Wu XD, Yang ZY, Jia P, Sun YQ, Li G, Xie L, et al (2019) Effects of paclitaxel intervention on pulmonary vascular remodeling in rats with pulmonary hypertension. *Exp Ther Med* **17**, 1163–1170.
18. Saari M, Vidgren MT, Koskinen MO, Turjanmaa VM, Nieminen MM (1999) Pulmonary distribution and clearance of two beclomethasone liposome formulations in healthy volunteers. *Int J Pharm* **181**, 1–9.
19. Nishimura T, Faul JL, Berry GJ, Vaszar LT, Qiu DM, Pearl RG, Kao PN (2002) Simvastain attenuates smooth muscle neointimal proliferation and pumonary hypertension in rats. *Am J Respir Crit Care Med* **166**, 1403–1408.
20. van den Akker J, VanBavel E, van Geel R, Matlung HL, Guvenc Tuna B, Janssen GM, van Veelen PA, Boelens WC, et al (2011) The redox state of transglutaminase 2 controls arterial remodeling. *PLoS One* **6**, e23067.
21. Penumatsa KC, Fanburg BL (2014) Transglutaminase 2-mediated serotonylation in pulmonary hypertension. *Am J Physiol Lung Cell Mol Physiol* **306**, L309–L315.
22. Yi B, Cui J, Ning JN, Wang GS, Qian GS, Lu KZ (2012) Overexpression of PKGIα inhibits hypoxia-induced proliferation, Akt activation, and phenotype modulation of human PASMCs: the role of phenotype modulation of PASMCs in pulmonary vascular remodeling. *Gene* **492**, 354–360.
23. Li GW, Xing WJ, Bai SZ, Hao JH, Guo J, Li HZ, Li HX, Zhang WH, et al (2011) The calcium-sensing receptor mediates hypoxia-induced proliferation of rat pulmonary artery smooth muscle cells through MEK1/ERK1,2 and PI3K pathways. *Basic Clin Pharmacol Toxicol* **108**, 185–193.
24. Liu T, Jin H, Ullenbruch M, Hu B, Hashimoto N, Moore B, McKenzie A, Lukacs NW, et al (2004) Regulation of found in inflammatory zone 1 expression in bleomycin-induced lung fibrosis: role of IL-4/IL-13 and mediation via STAT-6. *J Immunol* **173**, 3425–3431.
25. Penumatsa K, Abualkhair S, Wei L, Warburton R, Preston I, Hill NS, Watts SW, Fanburg BL, et al (2014) Tissue transglutaminase promotes serotonin-induced AKT signaling and mitogenesis in pulmonary vascular smooth muscle cells. *Cell Signal* **26**, 2818–2825.